Quaternary International 438 (2017) 65–79

Contents lists available at ScienceDirect

Quaternary International

journal homepage: www.elsevier.com/locate/quaint

Quaternary-active thrusts scarps tested as deformation markers by trishear models in the Southern Precordillera of Argentina

Fabricio R. Vázquez [a, b], Carlos H. Costa [a, *], Carlos E. Gardini [a]

[a] Departamento de Geología, Universidad Nacional de San Luis, E. de los Andes 950, 5700, San Luis, Argentina
[b] CONICET, CCT-San Luis, A. Brown 907, 5700, San Luis, Argentina

ARTICLE INFO

Article history:
Available online 13 August 2016

Keywords:
Precordillera
Argentina
Trishear models
Quaternary thrusts
Scarps

ABSTRACT

Scarps related to Quaternary-active thrust splays propagating in alluvial bajadas of the Southern Precordillera of Argentina (32°20′) were studied through detailed topographic surveys, in order to understand the reliability of these landforms as deformation markers at an outcrop scale. Geometric parameters of causative structures were used to constrain balanced cross-sections through trishear modelling for shortening estimation and also with the aim of comparing the predicted geometry of these models with the scarp profile. Shortening estimation through retro-deformation of scarps contours was also conducted as an alternative approach for calculating deformation affecting these alluvial surfaces.

Results indicate that fold geometries predicted by trishear modelling do not fit with the present scarp shapes, suggesting modifications and slope angle decrease of the front limb. In order to match the modelled folds with the scarp profiles, it is necessary to place constraints to fault parameters, such as ramp angle and tip point position, not compatible with field observations.

Trishear models predict shortening values 8 to 15 times larger than those obtained through line retrodeformation of scarp profiles. Therefore, scarp shapes at a mesoscopic scale in the study area, are not considered a reliable deformation marker for shortening estimation of propagating thrusts through an unconsolidated cover.

1. Introduction

In the southernmost section of the Pampean flat-slab of the Andes (31°–33°S), prominent Quaternary deformation and ongoing seismicity at the back arc is concentrated along the eastern piedmont of the Argentine Precordillera (Jordan et al., 1983; Ramos, 1988; Costa et al., 2000, 2006; Ramos et al., 2002; among others). A significant part of the Quaternary tectonic activity in the Southern Precordillera is related to the range-bounding Las Peñas Thrust (LPT) (Fig. 1), which overrides Neogene clastic rocks against Quaternary alluvial sediments (Cortés and Costa, 1996; Costa et al., 2000, 2005, 2014; Schmidt et al., 2011, 2012).

Significant stream downcutting across the LPT trace, allow to examine at outcrop scale one of the best Quaternary thrusting exposures along the entire Andean front. However, reliable stratigraphic markers are rarely present in the Quaternary alluvial layers, precluding an appropriate correlation between the shortening induced by this structure in the alluvial cover, with the resulting topographic signature.

The LPT usually exposes several blind foot-wall splays propagating into the Quaternary sediments, giving rise to fold-limb scarps in the piedmont environment (Fig. 2) (Costa et al., 2000, 2014). The deformed alluvial surfaces overlying these propagating splays are considered to be better suited for quantifying the thrusts-related deformation in the alluvial cover. These types of surfaces have been used as finite strain markers in many active contractional settings (Avouac et al., 1993; Bullard and Lettis, 1993; Mueller and Suppe, 1997; Benedetti et al., 2000; Dolan et al., 2003; Ishiyama et al., 2004, 2007; Davis et al., 2005; Gold et al., 2006; Lin et al., 2007; among others).

Evolutionary paths and resulting signatures of scarps related to propagating thrusts, either emergent or blind, are more complex and far less known than landforms resulting from other types of faulting. The lack of a free-face expressing the primary fault surface and the high variability in landforms related to the causative structure, are thought to be the main reasons (McCalpin and Carver, 2009). Thus, it is relevant to understand to what extend the present day morphologic signature of these scarps may constitute

* Corresponding author.
E-mail address: costa@unsl.edu.ar (C.H. Costa).

http://dx.doi.org/10.1016/j.quaint.2016.06.020
1040-6182/

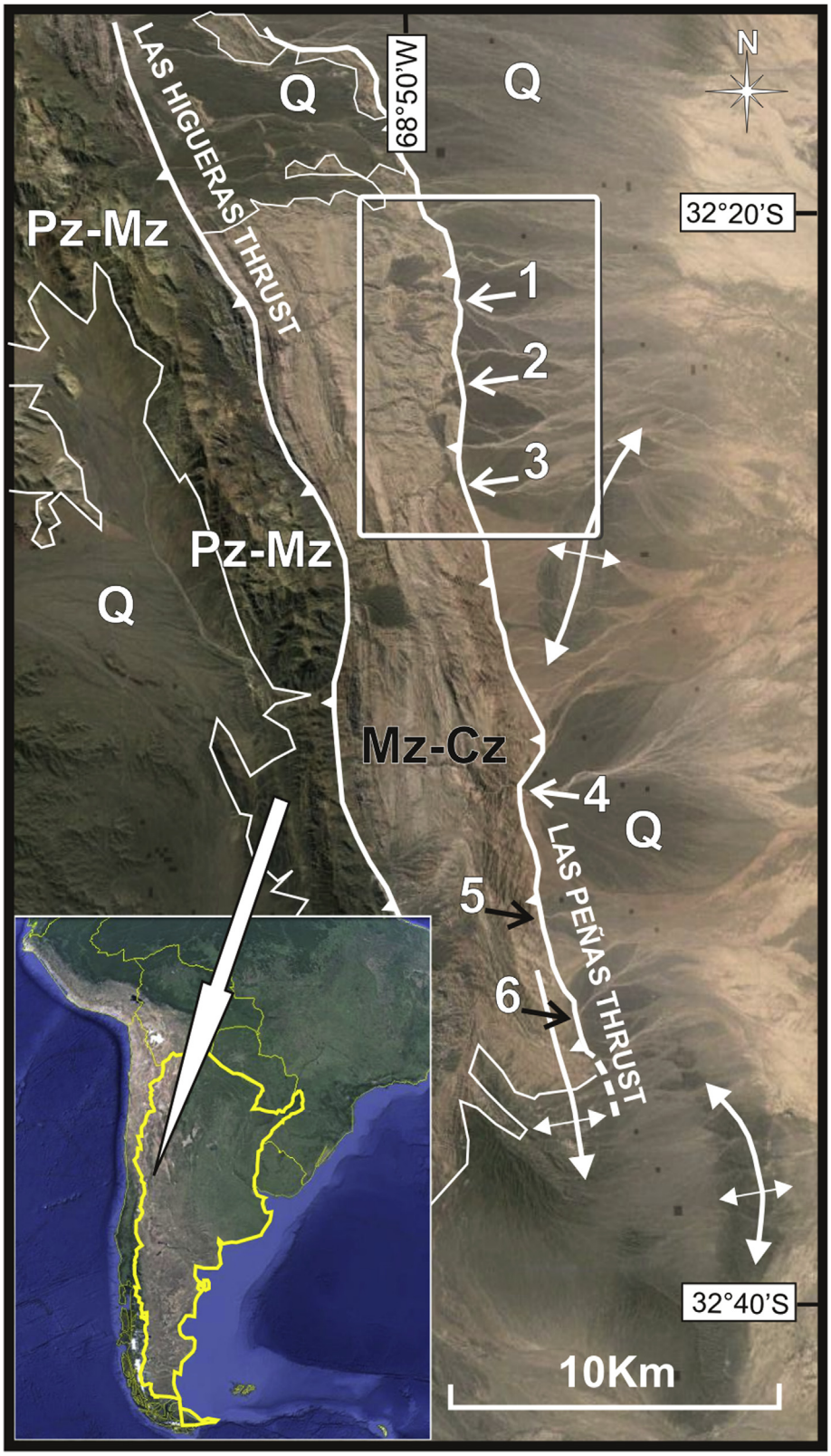

Fig. 1. Satellite view (Google Earth) of the Las Peñas-Las Higueras range area. Pz-Mz, Paleozoic–Mesozoic rocks; Mz-Cz, Mesozoic–Cenozoic rocks; Q, Quaternary alluvial cover. White rectangle corresponds to the study area showed in Fig. 2. Numbers refer to the creeks where scarps were profiled (1, Las Mañeras; 2, Infiernillo; 3, El Cóndor) or mentioned in the manuscript (4, Las Peñas; 5, La Escondida; 6, Baños Colorados). Folds identified in the piedmont environment are also depicted (Costa et al., 2000, 2014; Cortés et al., 2011). Inset shows the location of the study area in central-western Argentina.

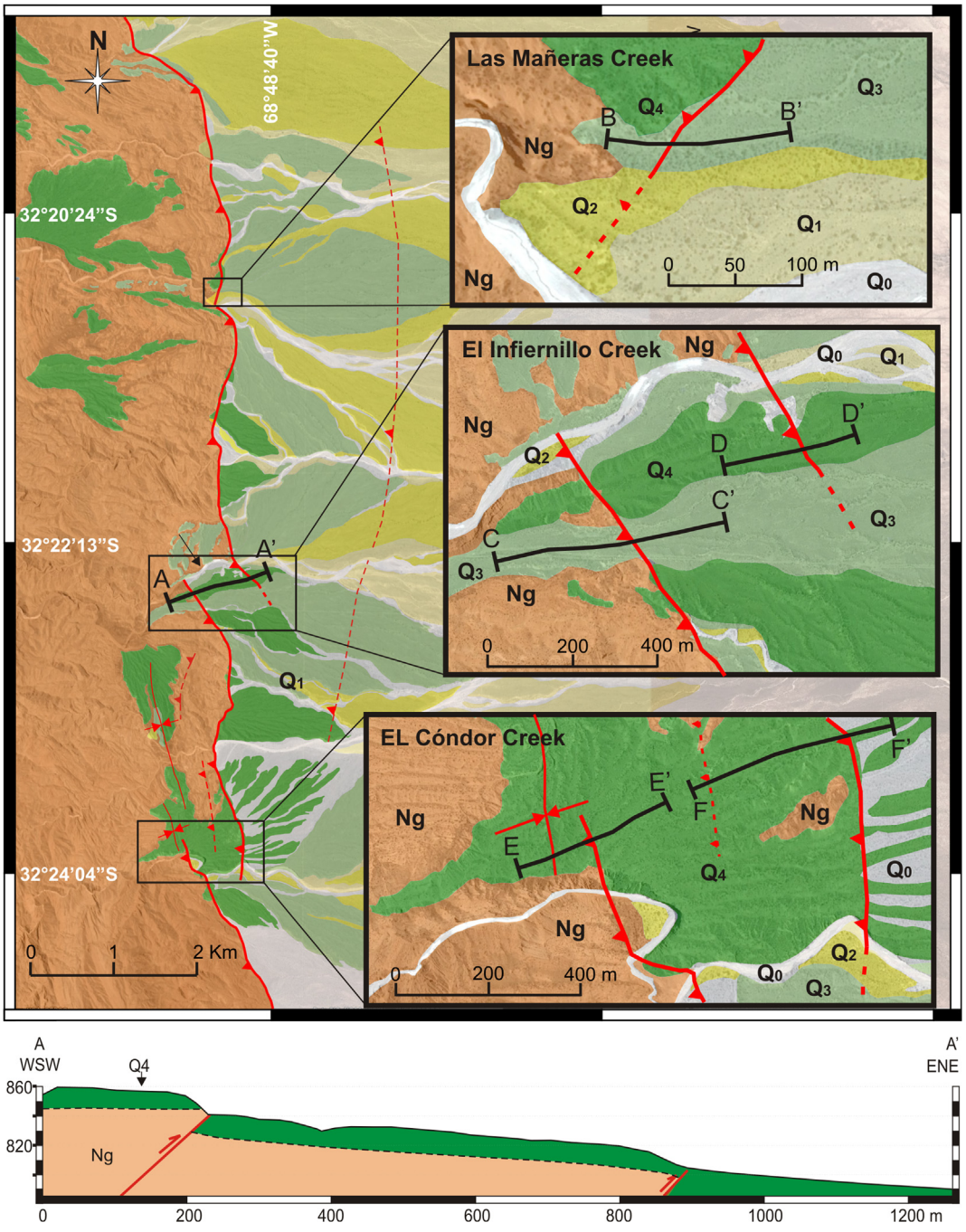

Fig. 2. Geological sketch of the study area with main lithologic units recognized and the main traces and structures related to the Las Peñas thrust shown with solid red lines (observed) and with dashed lines (inferred). Insets show the location of the surveyed scarps and profiles displayed in Figs. 7 (B–B′); 8 (C–C′); 9 (D–D′); 10 (E–E′) and 11 (F–F′). Profile A–A′ shows a schematic view of the LPT splays at the El Infiernillo creek, where the contact between the bedrock and Q_4 unit (dashed line) has been estimated for the most part. See the manuscript for details. (For interpretation of the references to colour in this figure legend, the reader is referred to the web version of this article.)

deformation markers of the thrust-related deformation, at detailed (decametric) scales.

A direct way to estimate shortening is to restore by line balancing the current scarp profile, assuming the selected surface being synchronous at both thrust walls. Under this approach, a fold-limb scarp is ascribed to a parallel type of folding, presuming that no significant internal shear or changes in layer thickness have taken place and requiring the scarp profile to be representative of the underlying fold geometry. These methods also assume that landform has not undergone modifications by erosion or other slope processes. This last requirement implies to decouple the topographic expression of a propagating structure, from possible interactions with exogenous processes.

Field observations in the study area as well as on other thrusts at the Southern Precordillera, indicate that Quaternary layers involved in thrust propagation do not behave as isopach-parallel folds at a decametric scale (Costa et al., 2000, 2014; Ahumada and Costa, 2009; Schmidt et al., 2011; Salomon et al., 2013). Thus, constraining the deformation related to these propagating thrusts solely based on the scarp topographic contour, can account for the uplift

produced by the fault slip, but may result in discrepancies regarding shortening and total slip estimation related to the causative structure.

Mechanical and numerical models as well as classical sand-box experiments, predict significant discrepancies between the inner geometry of folding related to propagating thrusts in comparison with the shape of the uppermost deformed layers (in this case the topographic surface) (Johnson and Johnson, 2002; Cardozo et al., 2003; Hardy and Finch, 2007; Hardy and Allmendinger, 2011; Takao et al., 2014; http://criepi.denken.or.jp/jp/kenkikaku/report/detail/N10049.html, last accessed December 2015; https://rocktraumacenter.wikispaces.com/2010+Compressional+Models, last accessed December 2015). This fact has also been underlined by historic surface ruptures (Kelson et al., 2001; Lee et al., 2004; Liu-Zeng et al., 2009) and is particularly relevant for moderate-low angle thrusts propagating into a detached and isotropic cover (Johnson and Johnson, 2002).

Several contributions have used the surface and shallow expression of Quaternary-active thrusts, through topographic and subsurface data at a macroscopic scale, as a geometric constrain for matching geometries derived from balanced cross-sections (Mueller and Suppe, 1997; Ishiyama et al., 2004, 2007; Gold et al., 2006; among others). We have here followed an inverse approach, aiming to test whether or not surveyed alluvial surfaces constitute reliable strain markers. Based on detailed topographic mapping and outcrop data, we investigate if morphological signatures of thrusts propagating into Late Pleistocene alluvial sediments can be reconciled with balanced sections for shortening estimation. Accordingly, shortening obtained by trishear models were contrasted against data resulting from line restoration of scarps profiles, in order to address how much the discrepancies between both approaches, if any, may impact in shortening estimation. This contribution also seeks to explore independent criteria for evaluating the modification degree of thrust-related scarps in unconsolidated alluvial deposits, in this kind of tectonic setting and working scale.

2. Morphotectonic setting

The study area is located at the southern part of the Precordillera, a Paleozoic orogen whose Neogene evolution has resulted in different neotectonic deformation styles, controlled by the inheritance of pre-Cenozoic structures. At the Southern Precordillera (Fig. 1) the Andean orogenic front is expressed by NNW-trending east-verging thrusts, being the best exposures of Quaternary-active structures concentrated at the Las Peñas-Las Higueras range. The western part of the range is made up of Paleozoic rocks, thrusted against Mesozoic and Cenozoic strata through the Quaternary-active Las Higueras Thrust (LHT) (Ahumada and Costa, 2009; Ahumada, 2010; Costa et al., 2015) (Fig. 1).

The LPT concentrates the most recent deformation along the range front, thrusting Neogene sediments over Quaternary conglomerates (Cortés and Costa, 1996; Costa et al., 2000, 2005, 2014; Schmidt et al., 2011). This thrust becomes blind at the southern tip of the range, giving rise to south-plunging folds which deforms the Neogene deposits (Costa et al., 2000, 2014; Cortés et al., 2011) (Fig. 1).

The thrust sheet comprised between the LHT and LPT traces exhibits a landscape dominated by a degraded erosion surface, partly covered by alluvial deposits. It is understood that continued Quaternary uplift has induced bedrock erosion, with subsequent deposition of fanglomerates, the older ones perched atop of this planation surface and the younger nested within the main creeks (Costa et al., 2000, 2014).

The tip zone of the LPT has evolved during the Quaternary in a close relationship with alluvial sedimentation. Progressive unconformities in association with propagating faults are exposed at the Las Mañeras creek, as clear examples of these processes (Costa et al., 2000, 2014). In contrast, foot-wall deposits exhibit little or no disturbance at all (Cortés and Costa, 1996; Costa et al., 2000, 2005, 2014; Ahumada and Costa, 2009; Ahumada, 2010). Uppermost deformed Quaternary alluvial layers across the LPT trace commonly show warping and monocline geometries consistent with fold-limb type of scarps, reaching sometimes the forelimb layers a vertical position (Costa et al., 2000, 2014). The lack of continuous exposures across the thrust-related scarps, a persistent debris cover and a poorly defined layering in the Quaternary deformed sediments, prevents a proper comparison and correlation between the profiles of scarps and the geometries of thrusted layers, exposed few meters below the topographic surface. Thus, in some cases it is difficult to judge if the thrust tip has broken the surface, giving rise to a hanging-wall collapsed scarp (McCalpin and Carver, 2009) or if fold-limb scarps still prevail instead.

At the LPT foot-wall, extensive deposits of quaternary fanglomerates make up the wide piedmont area in a typical alluvial fan environment, being data about their thicknesses poorly known to present (Figs. 1 and 2). No numerical ages have been so far reported in the study area, although data obtained in the main alluvial terraces at Las Peñas, La Escondida and Baños Colorados creeks (Fig. 1) have resulted in ages ranging from ~3,3 ka to ~123 ka for the oldest preserved alluvial surfaces (Schmidt et al., 2011, 2012; Schoenbohm et al., 2013).

It is hypothesized that the original enveloping alluvial surface might have been modified across these thrust-related scarps, mainly considering a non-steady piedmont morphodynamics during Late Pleistocene climate changes (Hedrick et al., 2013). Gravity-related slope modifications due to scarp diffusion and mass transfer could have also attenuated scarp morphology, eventually linked to successive fault slip events, even without significant erosion of the thrust-related front limb. To the east of the thrust front, stream incision has given rise to terrace formation within the fanglomerate deposits. Stream downcutting and widening has resulted in characteristic wing-like shapes. Entrenched meanders in the alluvial fan environment, either active or abandoned, testify for runoff anomalies in the foot-wall, probably induced by blind foot-wall shortcuts (Vazquez et al., 2015).

The NW-trending LPT thrust (140°–170°) dips at surface with moderate to low angles (15°W–55°W) and it is cored by Cenozoic clastic rocks. Although there are no subsurface data available to suitably constrain its cumulated slip, Neogene bedrock exhibits ~25 m of dip slip over Quaternary alluvial fan deposits at the Las Peñas river (Fig. 1) (Cortés and Costa, 1996; Costa et al., 2000, 2005, 2014). The LPT behaves either as a blind or emergent structure as regards to the Quaternary alluvial cover, the latter situation observed nearby the main creeks. The migration pattern of the LPT deformation zone follows a forward–breaking sequence, being the westerly splays incorporated successively into the thrust hanging-wall (Cortés and Costa, 1996; Costa et al., 2000, 2014; Cortés et al., 2011). It is difficult to precise the location of Quaternary-active thrust traces where the alluvial cover has been partly or totally eroded, because no fault-related morphologies are preserved. Based on aerial images, low sun-angle oblique aerial views and field work, the Quaternary-active LPT traces recognized are sketched in Fig. 2.

Deformation propagated into the Quaternary alluvial cover, suggests a lobate pattern of the LPT in the study area, composed by two major splays, spatially related through a relay ramp array (Fig. 2). Table 1 shows morphometric information of surveyed scarps, as well as geometric parameters of the causative thrusts.

Table 1
Morphometric data of the surveyed scarps and thrust attitudes measured below them. The preferred ramp angle used for trishear modelling resulted from the most representative dip angles of outcropping thrust surfaces or from averaging dip angles of curviplanar surfaces.

	Las Mañeras	El Infiernillo west	El Infiernillo east	El Cóndor west	El Cóndor east
Scarp slope	17°	14,5°	13,5°	10°	18°
Scarp height (m)	4,70	6,17	12,90	7,80	28,50
Measured thrust attitude (right hand rule)	295°/29° 300°/35° 315°/49°	326°/39°	305°/40° 320°/47° 330°/56° 313°/48°	323°/39° 329°/58°	354°/41° 354°/21° 354°/33°
Preferred ramp angle	37°	39°	43°	49°	18°

3. Geology of the study area

Two main geologic and geomorphologic settings separated by the LPT deformation zone stand out in the study area (Figs. 1 and 2). The thrust hanging-wall is characterized by an erosive environment, where folded Neogene rocks (Mariño Fm.) crop out. Remaining patches of the alluvial cover show a discontinuous strip array along the LPT thrust trace. The high erodibility of the Neogene rocks has determined the preservation of small remains of the regional erosion surface which underlies the Quaternary deposits (Costa et al., 2000, 2014).

The Mariño Formation is composed by fine-medium grained sandstones, claystones and siltstones of light brown and reddish colors, showing evidences of intense deformation during the Neogene, particularly at the LPT deformation zone.

The LPT foot-wall corresponds to a bajada environment where alluvial Quaternary deposits crop out (Figs. 1 and 2). Three main wing-like coalescent alluvial fans stand out, where mostly unpaired cut-in-fill and strath terraces could be identified. Cartographic discrimination of morphostratigraphic unit is relatively simple at the proximal part of the alluvial fans due to a scissors-like array of the alluvial terraces, becoming more complex at the distal part. Relative heights, dissection degree and local attributes of alluvial surfaces were taken into account for unit correlation (Table 2).

bedding structures. But in general, planar fabrics are roughly defined and non-persistent at a decametric scale.

Graywackes clasts and boulders prevail in older units (50%–70%), accompanied with clastic (10%–30%), volcanic rocks (10%–20%) and less commonly limestones (<5%). It is noteworthy that the proportional presence of blocks (>1 m) of reddish and brownish sedimentites (Mariño Fm. and similar) as well as grain size, increases towards younger units (Q_1, Q_0). This change is noticeable in the appearance of the alluvial surfaces, which stand out with light tones in aerial images (Figs. 1 and 2).

Quaternary deposits are usually unconsolidated, except in fault zones where could be cemented by epigenetic carbonates or gypsum.

Unit Q_2 and younger units do not expose noticeable morphologic evidences of thrust propagation. However the drainage pattern exhibits incised meanders carved in older units (Q_3 and Q_4), suggesting evidences of ongoing blind tectonic activity in the thrust foot-wall (Vazquez et al., 2015).

A brief description of surface characteristics of these cartographic units is provided in Table 2.

4. Methods

The LPT section here analyzed was selected due to the occurrence of scarps related to thrust propagation in the piedmont al-

Table 2
Description of the surface characteristics of the morphostratigraphic units distinguished. See the manuscript and Fig. 2 for other details.

Unit	Distribution	Surface characteristics
Q_0	Both thrust walls	Corresponds to active channels. It exhibits high reflectance and light pinkish tones due to predominance of blocks and matrix of Neogene rocks.
Q_1	Thrust foot-wall	Low dissection degree and light pinkish tones. Smooth to slightly rough texture. It is nested within the older units in the proximal/apical zone of the alluvial environment, whereas it appears widely distributed in the eastern parts of the area (Figs. 1 and 2). This surface become functional during heavy floods and could be partly covered by overbanking deposits. No desert varnish present. Subrounded to rounded non-coated clasts, with average size of 2 cm (35% of the exposed surface).
Q_2	Preserved at the thrust foot-wall. Its aerial significance decreases from North to South	Grey tones and a less incised than older units. Clasts are subangular to subrounded with average size of 4 cm and desert varnish poorly developed.
Q_3	Few remains nested within main creeks at the hanging-wall, but largely prevail in the foot-wall.	Medium-high dissection degree, dark tones and rough texture. Good development of desert pavement, coating angular clasts of 4 cm-average (long axis maximum size is up to 1.5 m), which represent up to 30% of the coarse clastic fraction.
Q_4	Small patches at the LPT hanging wall and rarely present at the foot-wall.	Dark tones and the highest dissection degree. These strath terraces deposits exhibit the thickest layers exposed. Angular clasts (3 cm-average and 1.5 m-maximum) are dominant with a good development of desert pavement. Boulders represent ca. 20% of the alluvial Surface. Scarce limestone boulders show differential dissolution micromorphologies (limestone/chert) $\geq$ 7 mm.

Lithologic composition and aspect of the five Quaternary morphostratigraphic units distinguished is very similar, except when comparing oldest against youngest deposits. These sediments are constituted mostly by sheet-flood and debris flow deposits, uncomformably overlying the Mariño Formation (Figs. 3–5). They are predominantly made of dark grey to light brown (in the web version) colors, both clast or matrix supported, and a sandy matrix with variable proportion of fine gravels and silt. Where flood sheet fan prevail, a discrete layering is present, sometimes with cross-

luvial units, along with exposures of the shallow portion of the deforming structures in the main creeks (Figs. 3–5). Several sections for shortening estimation were targeted with alluvial surfaces outcropping at both thrust walls and interpreted as synchronous (Fig. 2).

Field mapping was assisted by aerial images and oblique photos of low-altitude flights. Detailed topographic surveys through kinematic GPS, were conducted in order to carefully identify morphostratigraphic units and to quantify scarp morphology. Selected

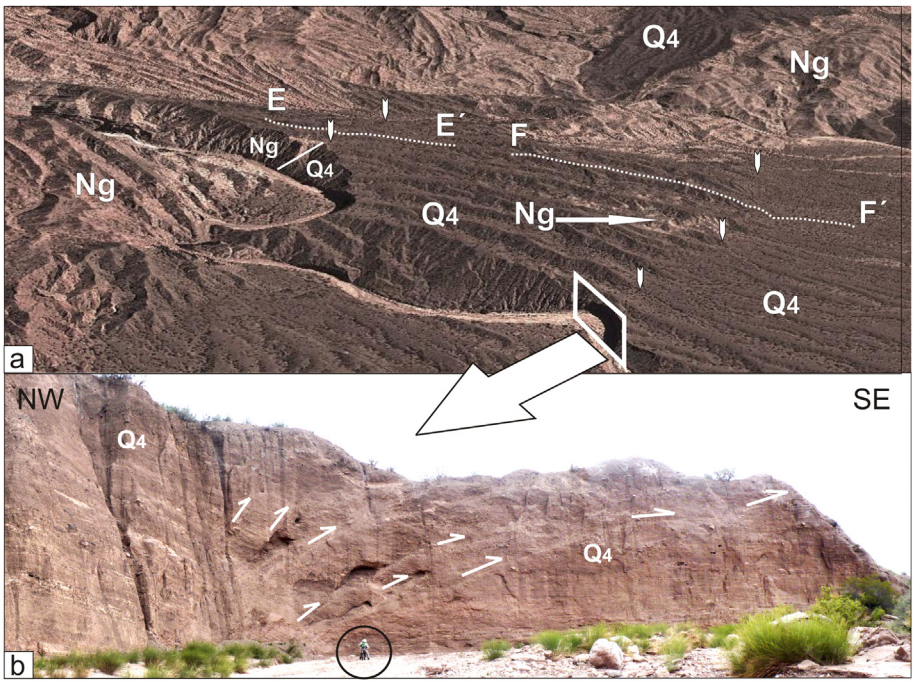

Fig. 3. Northwest-looking oblique aerial view of the El Cóndor creek (Fig. 3a). Scarps related with two splays of the LPT are indicated with white vertical arrows. E–E′ and F–F′ indicate the location of scarp profiles shown in Figs. 10 and 11. References for outcropping lithologic units are the same as in previous figures. White quadrangle corresponds to the location of Fig. 3b. White arrows here highlight propagating splays of the LPT (profile F–F′, Fig. 11). Note the dip variation of Q_4 layers at both sides of the deformation zone. Geologist within circle for scale.

cross sections were surveyed where rill incision was not observed or considered minimal as to the working scale (Figs. 2 and 3).

Non-parallel types of folding characterize the geometries of Quaternary deformation related to the LPT and surrounding structures (Ahumada and Costa, 2009; Ahumada, 2010; Schmidt et al., 2011, 2012; Salomon et al., 2013; Costa et al., 2015), as also exposed at the Las Mañeras creek (Fig. 8 in Costa et al., 2014). This fact prevents to construct balanced sections following the techniques proposed by Woodward et al. (1989) and Suppe and Medwedeff (1990). For that reason, trishear fault-propagation models were considered more appropriate for modelling the structures here described.

The trishear theory of fault-related folding was first described by Erslev (1991) and has subsequently been widely accepted (Hardy and Ford, 1997; Allmendinger, 1998; Zehnder and Allmendinger, 2000; Hardy and Allmendinger, 2011; among others). It relates fold geometry with faulting parameters assuming isotropic and homogeneous materials, allowing a good correlation with numeric mechanical models (Johnson and Johnson, 2002; Cardozo et al., 2003; Hardy and Finch, 2007). The coarse and barely unconsolidated gravels with poorly defined fabric and layering here described, could qualify for such mechanical conditions. We used a forward modelling procedure to test if the scarp profiles could be used as a reliable marker for shortening estimation, by comparing the surface deformation predicted by trishear with the internal and cumulated deformation in the Quaternary units with the scarp topography. Modelling was undertaken through the FaultFoldForward v.6.2.0 software (www.geo.cornell.edu/geology/faculty/RWA/programs/faultfoldforward.html; last accessed December 2015), in order to link scarp geometries and fault parameters with kinematically balanced sections.

The selected scarps profiles were displayed in the background of the computer screen. Then, a range of maximum and minimum values of parameters controlling the geometry of trishear folding (angle of trishear zone, ramp angle, tip point position, P/S ratio),

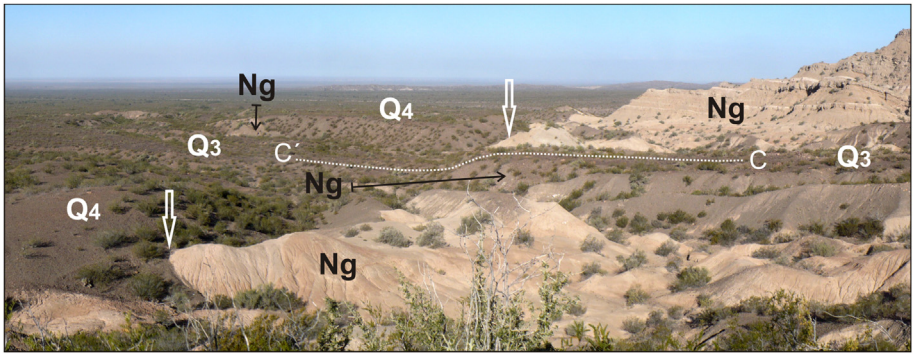

Fig. 4. Southeast-looking view of the western trace of the LPT at the El Infiernillo creek. Thrust location pinpointed with white arrows is suggested by the distribution of the Neogene (Ng) and Quaternary (Q_3, Q_4) units, although no diagnostic morphologies of Quaternary thrusting activity are preserved, except where Q_3 unit overlies both thrust walls. Scarp profile (C–C′) is shown in Fig. 8.

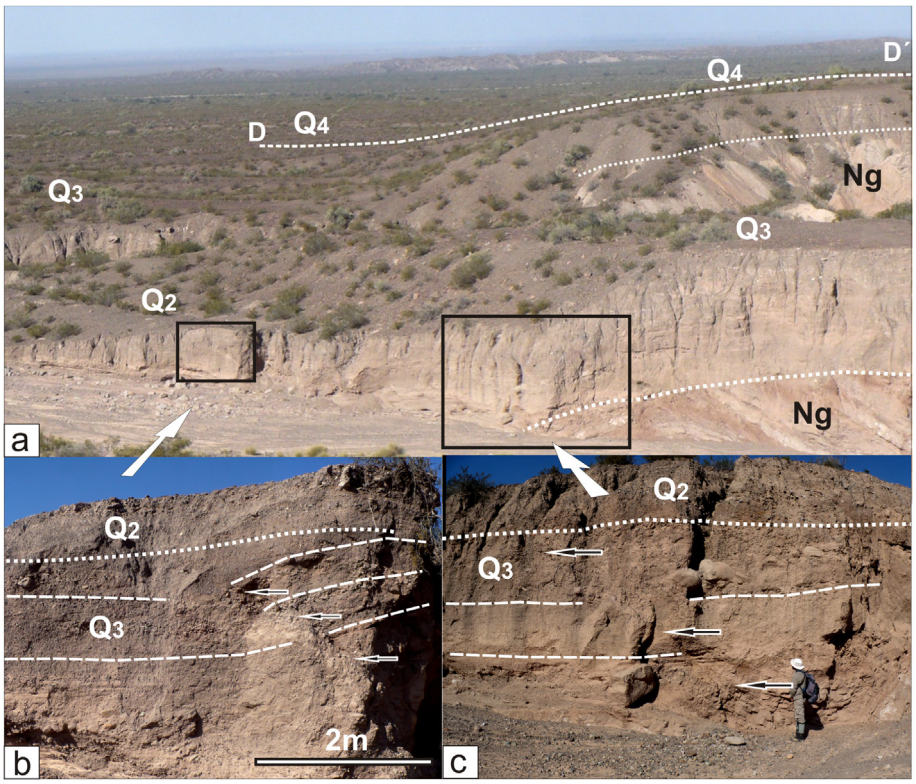

Fig. 5. a. Southeast-looking view of the scarp related to the LPT eastern splay at the El Infiernillo creek, indicating the location of profile D–D′ (Fig. 9). Outcrops of Neogene rocks (Ng) are visible at the hanging-wall. The gentle relief of a piedmont anticline can be seen in the background (see Fig. 1 for location). b and c displays details of propagating splays visible in Q_3 unit, but not affecting Q_2 unit sediments. Contacts between lithologic units are shown with white dotted lines, whereas poorly defined layering in Q_3 sediments is underlined with dashed lines. Arrows indicate the thrust surface.

either surveyed or estimated, were tested through a trial and error procedure, until finding the best fits between output models and scarp profile by visual inspection (Table 3). Markers provided by trishear models were matched to the regional slope of the topographic enveloping surface at the scarp far field, in order to avoid inconsistencies eventually introduced by scarp modification (Fig. 6).

topography, which encompasses in most cases the length of the entire cross section.

There is not too much empirical data regarding relations between the propagation/slip (P/S) ratio and the rheology of different materials. We have used P/S values ranging between 2,5 and 3 not only due to better fits obtained, but also because we assumed that the low consolidated gravels might be less efficient to propagate

Table 3
Parameters involved in fold geometries compatible with the scarps heights, obtained through forward trishear modelling. Tip point location for each model is referred above (+) or below (−) the foot-wall datum. Last two columns to the right show resulting shortening estimated through trishear and line restoration methods respectively.

Location		Ramp (fault angle)	Apical angle (trishear zone)	Propagation/ Slip ratio (P/S)	Slip (m)	Tip point location (m)	Initial horizontal length (m)	Final horizontal length (m)	Shortening -trishear (m)	Shortening -line restoration (m)
Las Mañeras	Fig. 8a	37°	60°	2.5	07.69	+4,70	426	419.85	6.15	0.77
	Fig. 8b	37°	60°	2.5	07.69	−2,04	426	419.85	6.15	
	Fig 6c	37°	100°	3	08.55	−3,22	426	421.34	4.66	
El Infiernillo west	Fig. 8a	39°	60°	2.5	11.96	+6,17	308	298.69	9.31	0.99
	Fig. 8b	39°	60°	2.5	11.96	At surface	308	298.69	9.31	
	Fig. 8c	39°	100°	3	12.82	−12,50	308	301.08	6.92	
El Infiernillo east	Fig. 8a	43°	60°	2.5	17.28	+12,60	616	603.41	12.59	1.53
	Fig. 8b	43°	60°	2.5	17.28	At surface	616	603.41	12.59	
	Fig. 8c	43°	100°	3	18.52	−33,00	616	606.49	9.51	
El Cóndor west	Fig. 9a	49°	60°	2.5	15.12	+7,24	418	408.08	9.92	1.04
	Fig. 9b	49°	60°	2.5	15.12	At surface	418	408.08	9.92	
El Cóndor east	Fig. 10a	18°	60°	2.5	80.67	+19,26	1679	1618.75	60.25	3.89
	Fig. 10b	18°	60°	2.5	72.27	At surface	1679	1625.05	53.95	
	Fig. 10c	18°	100°	3	72.27	−6,85	1679	1626.3	52.7	

Preferred ramp angle (fault dip) for each section was chosen considering the most representative value of measured thrust dips at a meso-macro scale, whereas the position of the tip point was constrained through field observations. The apical angle (trishear zone) was adjusted according to the best fits obtained with the

faults in comparison to brittle rocks (Hardy and Finch, 2007; Hardy and Allmendinger, 2011). Thrust-related shortening was also estimated for selected cross-sections by retrodeformation of the scarp profiles, in order to contrast results provided by both methods. Shortening here resulted from comparing the scarp contour along a

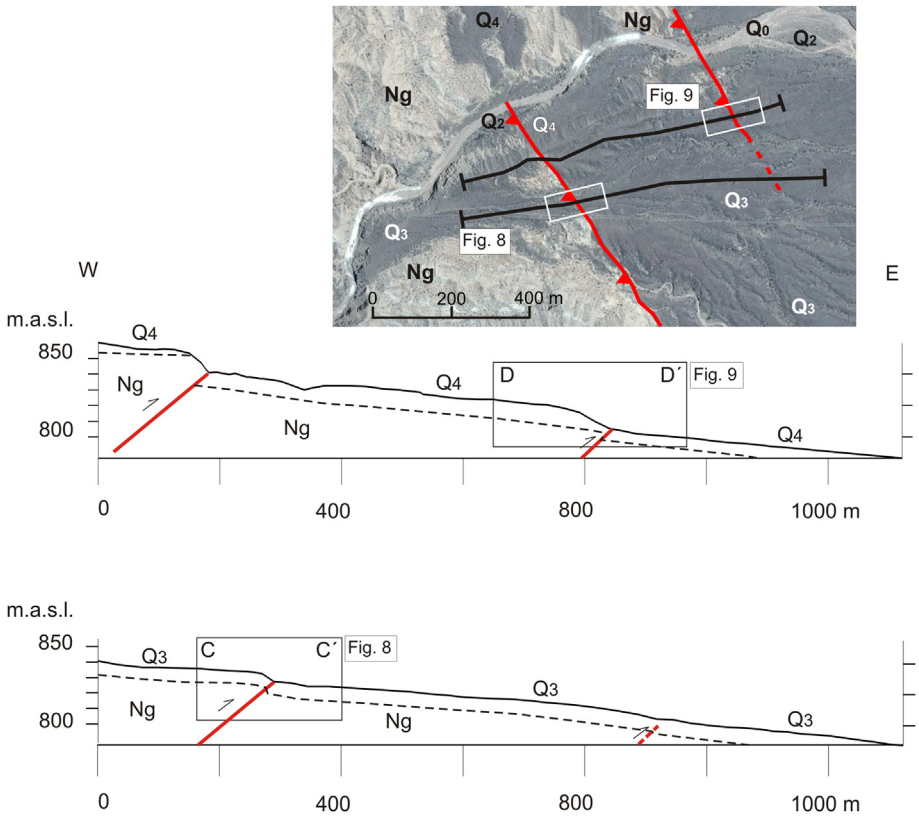

Fig. 6. Scarps profiles of deformed Q_3 and Q_4 surfaces (C–C′ and D–D′ respectively) and sketched geology at the El Infiernillo creek area. These cross-sections illustrate that even if trishear models only display the scarp zone for fitting details, they fit the far field slope of these alluvial surfaces. Inset with profiles location corresponds to the same image shown in Fig. 2.

specific length of each selected profile, against a straight-line with the same length. Results are also displayed in Table 3.

5. Shortening estimation through trishear modelling

5.1. Las Mañeras creek (profile B–B′, Fig. 2)

Only one section at an inset terrace (Unit Q_3) was selected at the Las Mañeras creek, because Q_4 unit was not properly preserved at the hanging-wall. In order to best capture the far field slope of this surface, a section slightly oblique (27°) to the thrust trace was chosen. However, the topography displayed in Fig. 7 corresponds to local sections profiled perpendicular to the structure trend at the scarp. Best fits in the regional slope were achieved through the parameters indicated in Table 3.

Fig. 7a predicts a lessening of the original scarp slope angle and a tip point above the topographic surface. On the south wall of Las Mañeras creek, thrusts splays concave downwards can be observed barely propagating up to the current datum of the preserved alluvial surface of Unit Q4 (Fig. 7 in Costa et al., 2014). Therefore, the preferred solution corresponds to a fault tip of the propagating fault near or above surface of Unit Q_3 (Fig. 7b). This implies to assume that the current scarp shape has undergone modifications, which results in discrepancies with the fold shape and related shortening.

Fig. 7c can reproduce the present scarp shape but requires a tip point to be placed 3.22 m below the present scarp base. Therefore, the fold shape fitting the topography does not represent the propagation stage of the causative structure and underestimates the cumulated shortening.

5.2. El Infiernillo creek west (profile C–C′, Fig. 2)

Field data indicate that fault tip should be near the surface of Unit Q_3 or even that the thrust might be already emergent (Fig. 4 and Table 3). Then, three different scenarios were here selected. Location of the fault tip nearby or above topographic surface, gives rise to significant discrepancies with the scarp profile (Fig. 8a and b). Trishear folding induced by the propagation of a fault dipping 39°W can perfectly fit the present scarp shape under different modelling parameters (Table 3 and Fig. 8c), but it requires the fault tip to be located 12.5 m below the outcropping Quaternary layers. This scenario does not satisfy the evidences of thrusting observed in the Quaternary deposits (Fig. 4). Accordingly models displayed in Fig. 8a and b are considered more consistent with field data. Regardless the option chosen, shortening predicted by trishear is the same in both cases, although larger than the one predicted by model showed in Fig. 8c (Table 3).

5.3. El Infiernillo creek east (profile D–D′, Fig. 2)

An eastern splay of the LPT affecting Q4 surface was here selected along a strip where this unit is still suitably preserved (Fig. 5a). Fig. 9a shows the fold geometry with a fault tip 12.6 m above the topographic surface, fitting the foot-wall slope and the hanging wall contour at the far field. This model implies to assume significant discrepancies between the present day scarp morphology, in comparison with the geometry predicted by the model.

Fig. 9b represents the situation with a fault tip at surface, which is well constrained with field data, but also implies significant scarp slope modification. Both options result in same shortening values (Table 3).

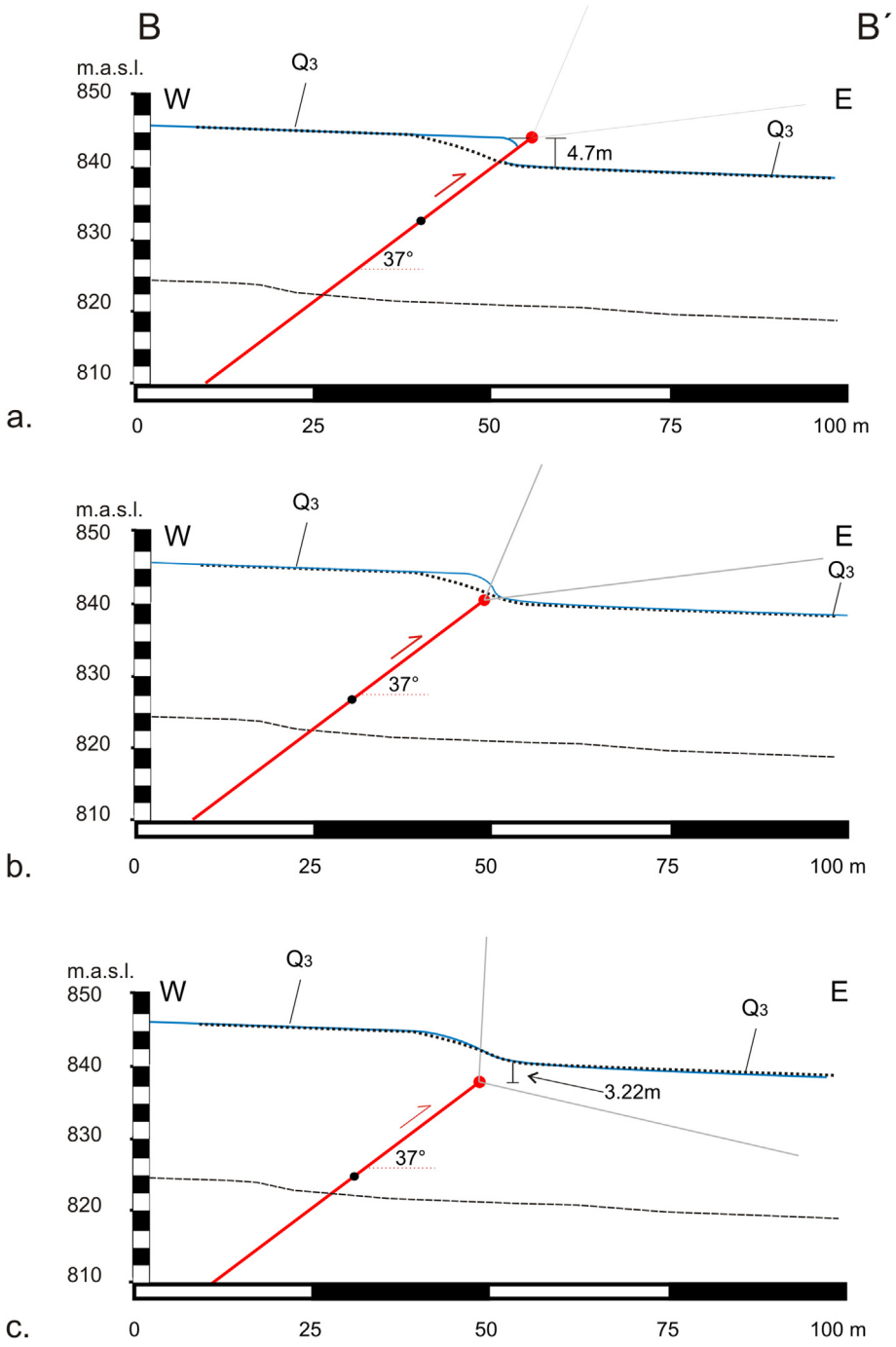

Fig. 7. Topographic profile B–B′ (dotted black line) of the scarp related to the LPT propagation in unit Q_3 at the Las Mañeras creek, sketching different thrust propagation scenarios. Blue lines correspond to selected geometries predicted by trishear models, under different modelling conditions. Black dashed line shows the river profile. Solid grey lines constrain the trishear angle; red and black dots are tip points and starting points respectively. See text and Table 3 for explanation. (For interpretation of the references to colour in this figure legend, the reader is referred to the web version of this article.)

Fig. 9c represents the best fit to the topographic surface. However, it requires to places the fault tip 33 m below the footwall datum of Q_4 Unit, meaning below the outcropping layers (see stream profile location in Fig. 9c). This model predicts folding instead of propagating faults at the surveyed outcrops. Hence, this option was not considered feasible according to field data.

The model represented by Fig. 9b is the preferred solution. It suggests a different shape of the fold forelimb in comparison with the present scarp shape, as well as a much larger shortening than predicted by retrodeforming the topographic surface (Table 3).

5.4. El Cóndor creek west (profile E–E′, Fig. 2)

Two traces of the LPT with surface expression were profiled nearby El Condor creek across alluvial surface represented by Unit Q4 (Fig. 3a).

The western trace shows an emergent thrust with a thin overlying alluvial cover nearby (Fig. 8 in Costa et al., 2014). This implies that the thrust surface might have either ruptured at surface or subsequently eroded (probably both situations apply). Accordingly, two models with the fault tip located above (Fig. 10a) and right on

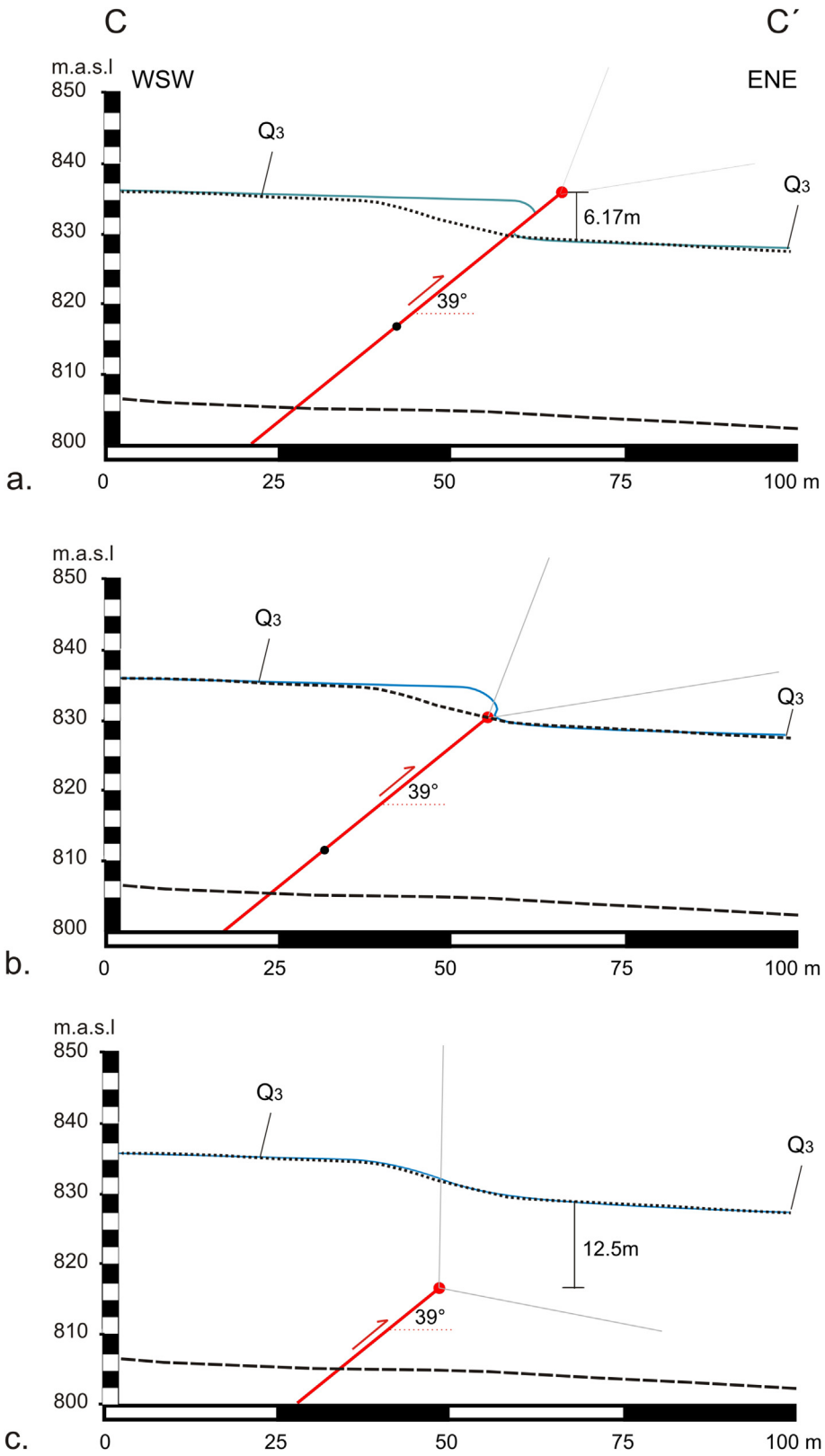

Fig. 8. Topographic profile C–C′ (dotted black line) of the scarp related to the western splay of the LPT (dotted black lines) in unit Q_3 at the El Infiernillo creek, sketching different thrust propagation scenarios. Blue lines correspond to selected geometries predicted by trishear models under different modelling conditions. Black dashed line shows the river profile. Solid grey lines constrain the trishear angle; red and black dots are tip points and starting points respectively. See text and Table 3 for explanation. (For interpretation of the references to colour in this figure legend, the reader is referred to the web version of this article.)

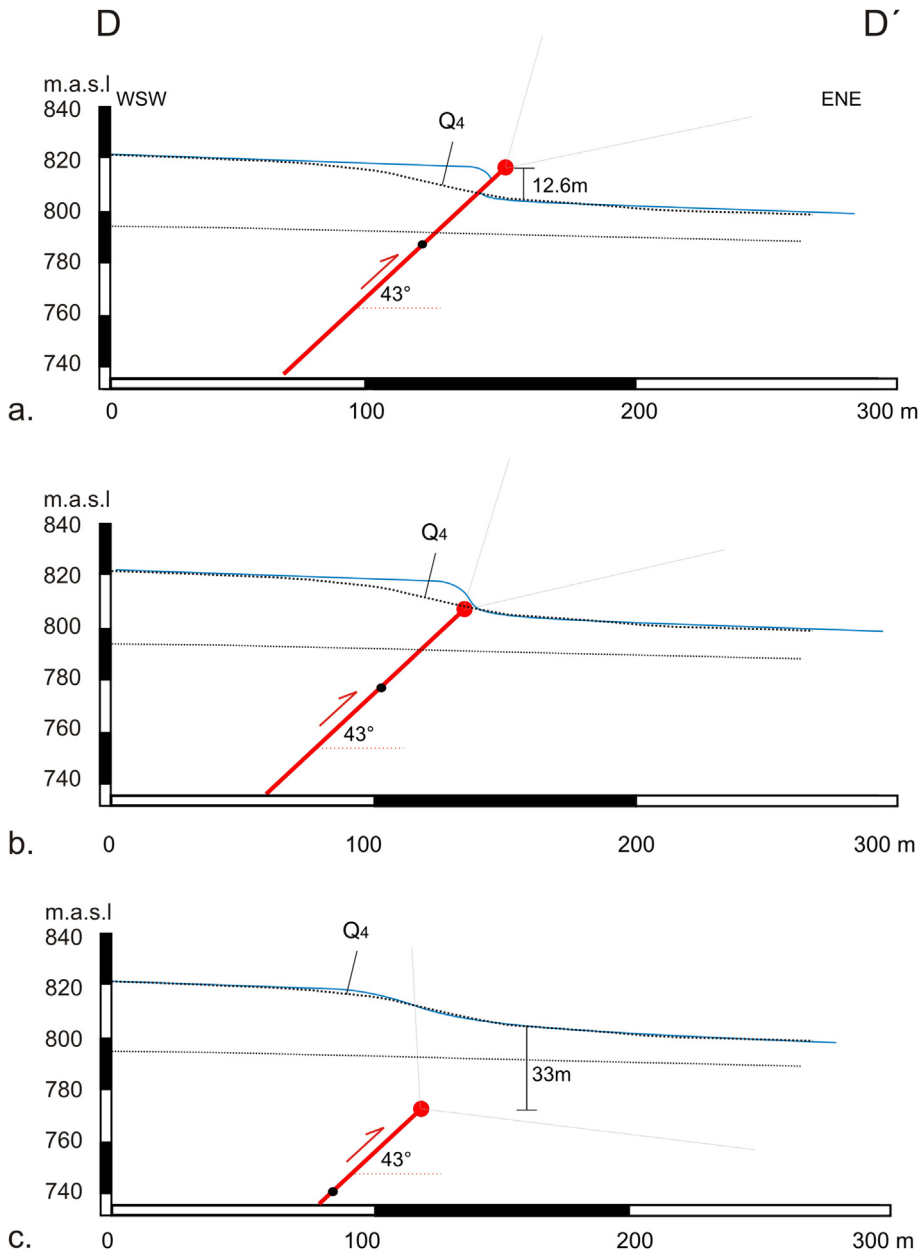

Fig. 9. Topographic profile D–D′ (black dotted line) of the scarp related to the eastern splay of the LPT in unit Q_4 at the El Infiernillo creek, sketching different thrust propagation scenarios. Blue lines correspond to selected geometries predicted by trishear models under different modelling conditions. Black dashed line shows the river profile. Solid grey lines constrain the trishear angle; red and black dots are tip points and starting points respectively. See text and Table 3 for explanation. (For interpretation of the references to colour in this figure legend, the reader is referred to the web version of this article.)

the surface are proposed as minimum thrust propagation scenarios (Fig. 10b). In agreement with field observations, the resulting models predict that the scarp has been modified and allow to constraint a probable scarp shape related to the cumulated thrust slip.

Because it is clear that the scarp has been already eroded, retrodeformation is not a valid option to estimate shortening. Difference of results between both methods is substantial (Table 3).

5.5. El Cóndor creek east (profile F–F′, Fig. 2)

The eastern trace of the LPT at El Cóndor creek also affects Q_4 Unit with low angle splays (Fig. 3b). The model depicted in Fig. 11a assumes that the thrust has already ruptured and propagated several meters above the alluvial surface in order to match the regional slope. Fig. 11b represents a scarp configuration considering the tip point at surface and Fig. 11c shows a perfect fit with the topography, being the fault tip located ~5 m above the longitudinal profile of the present stream channel.

Although it is not possible to accurately constrain the exact position of the fault tip, we favor the scenario depicted by Fig. 11b. Field observations suggest that fault tip is located very close to topographic surface because Neogene rocks barely crop-out at the hanging-wall (Fig. 3a). Debris talus deposits widely distributed preclude to refine this information. The thrust surface does not concentrate very evident shear phenomena along it (Fig. 3b), so we estimated a cumulated slip in the order of 1–10 m. This estimation is empirically-based, by comparing cumulated slip along with

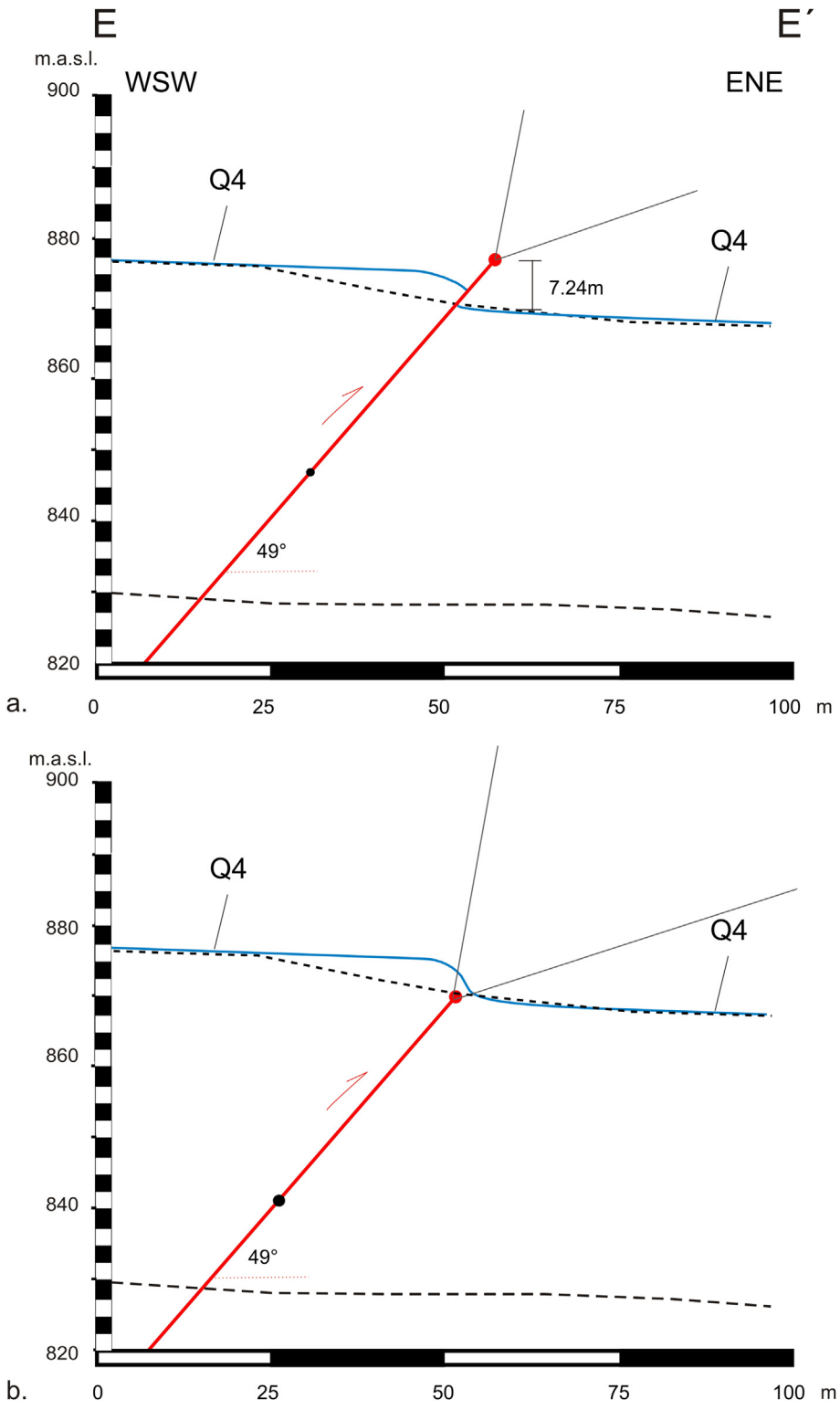

Fig. 10. Topographic profile E–E′ (black dotted line) of the scarp related to the western splay of the LPT in unit Q_4 at the El Cóndor creek, sketching different thrust propagation scenarios. Blue lines correspond to selected geometries predicted by trishear models under different modelling conditions. Black dashed line shows the river profile. Solid grey lines depict trishear angle. Red and black dots are tip points and starting points respectively. See text and Table 3 for explanation. (For interpretation of the references to colour in this figure legend, the reader is referred to the web version of this article.)

concentrated shear phenomena in other thrust splays outcropping nearby.

Several propagating splays concave downwards can be observed below the thrust scarp, subtly imposed on the alluvial fabric (Fig 3b), although their contribution to the overall scarp morphology and related shortening was not evaluated.

Model indicated in Fig. 11c cannot account for the evidences of fault traces observed at the creek walls (Fig. 3b), because folding

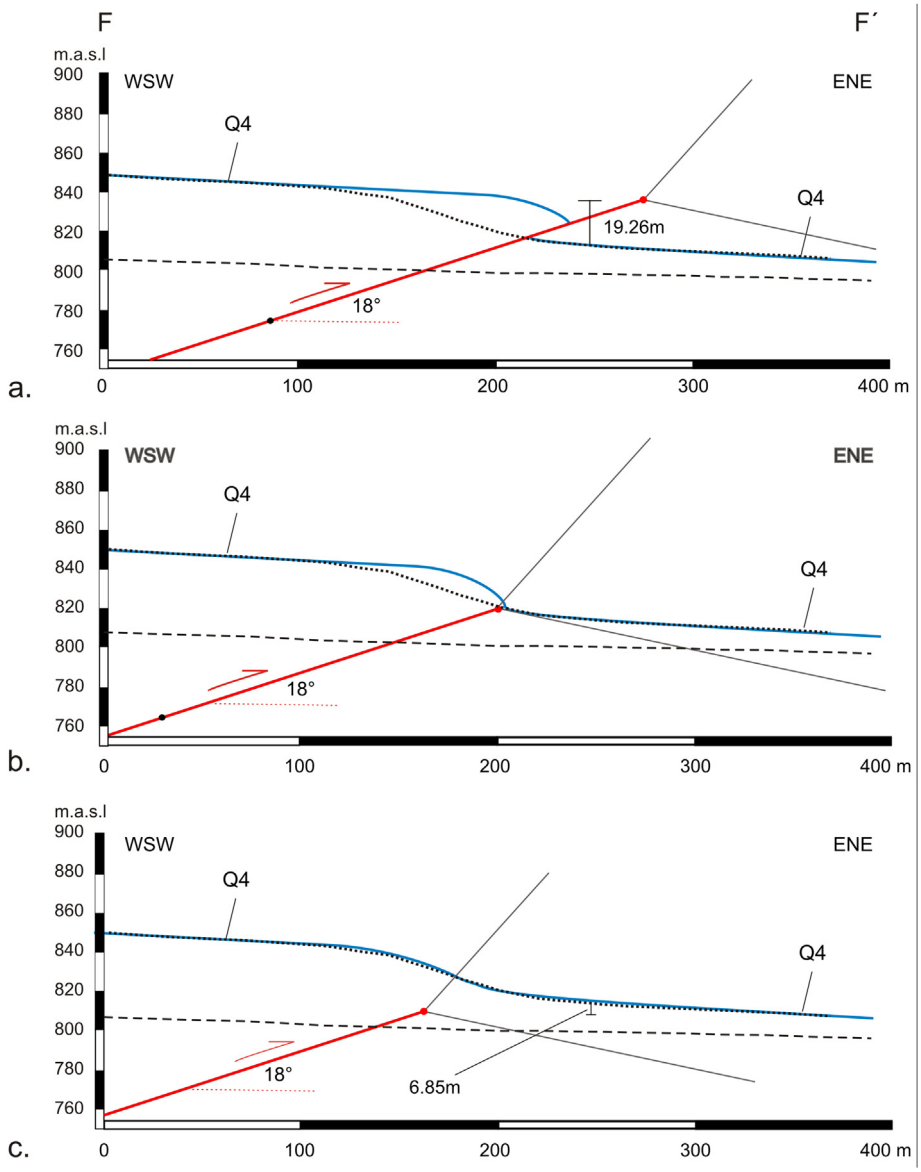

Fig. 11. Topographic profile F–F′ (black dotted lines) of the scarp related to the eastern splay of the LPT in unit Q_4 at the El Cóndor creek, sketching different thrust propagation scenarios. Blue lines correspond to selected geometries predicted by trishear models, under different modelling conditions. Black dashed line shows the river profile. Solid grey lines depict trishear angle. Red and black dots are tip points and starting points respectively. See text and Table 3 for explanation for explanation. (For interpretation of the references to colour in this figure legend, the reader is referred to the web version of this article.)

should be present instead. This result suggests that adjusting the fold geometry to the present surface is not a good approach to estimate shortening in this case. It also implies that scarp morphology has been modified in comparison to the fold shape predicted by the cumulated slip.

6. Discussion

Modelling fold propagation coupled with resulting morphologies requires to combines different kind of data and to consider different types of processes. We discuss below some issues arising from this case study.

Folds modelled through the trishear theory represent kinematically balanced geometries which match the vertical component of the cumulated thrust slip, constrained by the scarp topography. They can display discrepancies between the scarp contours and fold geometries of the total thrust slip accrued under different modelling conditions. The selected fold geometries may represent the pristine scarp shapes, if interactions between the fault propagation and the surface processes would have not taken place. For instance, the software utilized cannot model colluvial wedges and related slope deposits that might have been deposited at the scarp base. Accordingly, the models here presented are conceived as instruments for analyzing reliability of geomorphic surfaces as deformation markers, rather than an attempt to quantify scarp degradation or evolution.

The Fault/Fold v.6.2.0 software does not consider heterogeneous trishear and thus not all possibilities are here encompassed. The modelled thrusts takes into account a ‘basement’ (the pre-Quaternary lithified rocks) and a detached cover (the overlying alluvial sediments). This cover is poorly or non-consolidated, where layering is barely developed and no suitable mechanical discontinuities for developing layer-parallel slip are present.

At the El Infiernillo creek, balanced cross sections were developed in the oldest Quaternary unit preserved (Q_4) as well as in a younger inset terrace (Unit Q_3), being the shortening accrued larger in the former unit through both methods. These results suggest that thrust propagation has been contemporaneous with alluvial deposition, at least during the time elapsed between both units deposition. Thrust splays with submetric cumulated slip are present in the deposits of Q_3 unit (Fig. 5), although no noticeable morphologies derived has been detected in younger deposits. Thus, main thrusting activity seems to have taken place during the time period comprised between the deposition of these units.

It is worth to note that shortening estimated through trishear modelling have resulted in values eight to fifteen times larger than values obtained by line restoration of scarp profiles (Table 3). Maximum differences correspond to the El Cóndor East scarp (profile F–F′, Fig. 11). It is understood that the low angle of thrusting (18°) and scarp height are the main controlling parameters of the outstanding discrepancy at this site.

Costa et al. (2015) estimated the shortening related to a Holocene-active trace of the LHT, also through trishear and line retrodeformation techniques, but using deformed layers as markers for balancing, instead of the scarp profile. Results derived from both methods were similar, probably because of the layer-parallel stretching undergone by strata and avoidance of the thrusting bulldozing effect on topography. Therefore, significant discrepancies in shortening estimation should be expected when comparing the results obtained by retrodeforming the scarp profile as a strain marker, with the deformation accrued by underlying layers of the Quaternary cover, as also underlined by mechanical and experimental models (Johnson and Johnson, 2002; Takao et al., 2014). These discrepancies become even larger when the thrust surface tends to flatten upwards and scarp bulldozing becomes important in the resulting morphology (Kelson et al., 2001).

At the study area, trishear models have followed simple thrust geometries, which do not consider the complexities observed in the field, particularly referred to the upward decrease in dip angles and the thrust propagating in several splays (Fig. 3 in Costa et al., 2014). Variables introduced by these situations have not yet been explored. Nonetheless, it is understood that this approach allows to tests how representative a scarp shape could be from underlying causative structures, whose main parameters near surface are known.

7. Conclusions

In the study area, thrust-related landforms coined in Late Pleistocene alluvial surfaces are not considered reliable markers of the deformation accrued by propagating thrusts underneath. Restoration of topographic contours of scarps result in a considerable underestimation of the thrust-related shortening, when compared with results provided by balanced cross-sections. Shortening estimated through trishear modelling has resulted eight to fifteen times larger than values obtained by retrodeforming the scarp contour (Table 3).

Accordingly, finding the best fit between tectonic landforms and the causative thrusts using either numerical models or line retrodeformation is not an advisable procedure for estimating shortening at a decametric scale in the study area (See Figs. 7–11 and Table 1 for details).

Results obtained cannot account for all possible scenarios derived from fault-propagation folding, taking into account a combination of external factors, such as progressive slope modification, so as to intrinsic deformation processes of the unconsolidated layers.

Deformation propagating up to the uppermost layers of the terrace sediments, usually results in non-parallel type of folding, as documented in the area and outcrops nearby (Costa et al., 2000; Ahumada and Costa, 2009; Schmidt et al., 2011; Salomon et al., 2013; Costa et al., 2015). Scarp bulldozing due to flat-lying thrusting at surface, also enhances geometric discrepancies between scarp contours and folded layers of the alluvial cover underneath, which has a direct impact in shortening estimation through line restoration.

The line-restoration method does not consider stretching of folded layers. This fact may also help to explain significant differences in shortening results when comparing this approach with trishear models. Other structure parameters enhancing discrepancies between these methods are considered to be the surficial tip point location; low ramp angles (<30°) and unconsolidated and poorly layered materials of the thrust cover.

It is understood that balanced cross-sections of scarp morphologies through trishear models constitute an independent and sound approach for testing the reliability of scarps as strain markers of propagating thrusts at detailed (decametric scales). It contributes for a better understanding of relations between the cumulated thrust slip (constrained by its vertical component) and associated landforms.

Acknowledgements

We thank F. Hongn and an anonymous reviewer for constructive and thoughtful reviews. We are also indebted to E. Ahumada for sharing discussions and field work and V. Montenegro for field assistance. This work was supported by Universidad Nacional de San Luis (P. 320714).

Appendix A. Supplementary data

Supplementary data related to this article can be found at http://dx.doi.org/10.1016/j.quaint.2016.06.020.

References

Ahumada, E., 2010. Neotectónica del frente orogénico andino entre los 32°08′S – 32°19′S, provincias de Mendoza y San Juan (PhD thesis). Depto. Geología, Univ. Nac, San Luis.

Ahumada, E., Costa, C., 2009. Antithetic linkage between oblique Quaternary thrusts at the Andean front, Argentine Precordillera. Journal of South American Earth Sciences 28, 207–216. http://dx.doi.org/10.1016/j.jsames.2009.03.008.

Allmendinger, R., 1998. Inverse and forward numerical modeling of trishear fault propagation folds. Tectonics 17 (4), 640–656.

Avouac, J.-P., Tapponnier, P., Bai, M., You, H., Wang, G., 1993. Active thrusting and folding along the Northern Tien Shan and Late Cenozoic rotation of the Tarim relative to Dzungaria and Kazakhstan. Journal of Geophysical Research 98 (B4), 6755–6804.

Benedetti, L., Tapponnier, P., King, G., Meyer, B., Manighetti, I., 2000. Growth folding and active thrusting in the Montello region, Veneto, northern Italy. Journal of Geophysical Research 105, 739–766.

Bullard, T., Lettis, W., 1993. Quaternary fold deformation associated with blind thrust faulting, Los Angeles Basin, California. Journal of Geophysical Research 98, 8349–8369.

Cardozo, N., Bhalla, K., Zehnder, A., Allmendinger, R., 2003. Mechanical models of fault propagation folds and comparison to the trishear kinematic model. Journal of Structural Geology 25, 1–18. http://dx.doi.org/10.1016/S0191-8141(02)00013-5.

Cortés, J., Costa, C., 1996. In: Tectónica Cuaternaria en la desembocadura del Río de las Peñas, Borde oriental de la Precordillera de Mendoza, presented at the 13rd Congreso Geológico Argentino, vol. 2, pp. 225–238.

Cortés, J., Pasini, M., Prieto, C., 2011. In: Propagación y migración de la estructura cuaternaria del frente montañoso precordillerano en la sierra de Las Peñas, Mendoza, presented at the 18th Congreso Geológico Argentino, pp. 723–724.

Costa, C., Diederix, H., Gardini, C., Cortés, J., 2000. The Andean orogenic front at Sierra de Las Peñas-Las Higueras, Mendoza, Argentina. Journal of South American Earth Sciences 13, 287–292.

Costa, C., Gardini, C., Diederix, H., 2005. In: Tectónica vs. sedimentación en el Río de Las Peñas, Precordillera de Mendoza, presented at the 16th Congreso Geológico Argentino, La Plata.

Costa, C., Audemard, F., Becerra, F., Lavenu, A., Machette, M., París, G., 2006. An overview of the main Quaternary deformation of South America. Revista de la Asociacion Geologica Argentina 61 (4), 461–479.

Costa, C., Ahumada, E., Gardini, C., Vazquez, F., Diederix, H., 2014. Quaternary shortening at the orogenic front of the Central Andes of Argentina (32°15′-32°40′S): a field survey of the Las Peñas thrust. In: Sepúlveda, S., Giambiagi, L., Moreiras, S., Pinto, L., Tunik, M., Hoke, G., Farías, M. (Eds.), Geodynamic Processes in the Andes of Central Chile and Argentina, Geol. Soc. Special Publ. 399. http://dx.doi.org/10.1144/SP399.5.

Costa, C., Ahumada, E., Vazquez, F., Kröhling, D., 2015. Holocene shortening rates of an Andean-front thrust, Southern Precordillera, Argentina. Tectonophysics 664, 191–201. http://dx.doi.org/10.1016/j.tecto.2015.09.017.

Davis, K., Burbank, D., Fisher, D., Wallace, S., Nobesc, D., 2005. Thrust-fault growth and segment linkage in the active Ostler fault zone, New Zealand. Journal of Structural Geology 27, 1528–1546.

Dolan, J., Christofferson, S., Shaw, J., 2003. Recognition of paleoearthquakes on the Puente Hills blind thrust fault, California. Science 300, 115–118.

Erslev, E., 1991. Trishear fault-propagation folding. Geology 19, 617–620.

Gold, R., Cowgill, E., Wang, X., Chen, X., 2006. Application of trishear fault-propagation folding to active reverse faults: examples from the Dalong Fault, Gansu Province, NW China. Journal of Structural Geology 28, 200–219.

Hardy, S., Finch, E., 2007. Mechanical stratigraphy and the transition from trishear to kink-band fault-propagation fold forms above blind basement thrust faults: a discrete element study. Marine and Petroleum Geology 42, 75–90. http://dx.doi.org/10.1016/j.marpetgeo.2006.09.001.

Hardy, S., Ford, M., 1997. Numerical modeling of trishear fault propagation folding. Tectonics 16, 841–854.

Hardy, S., Allmendinger, R., 2011. Trishear: a review of kinematics, mechanics, and applications. In: McClay, K., Shaw, J., Suppe, J. (Eds.), Thrust Fault-related Folding, Am. Assoc. Petrol. Geol. Memoir 94, pp. 95–119. Tulsa.

Hedrick, K., Owen, L., Rockwell, K., Meigs, A., Costa, C., Ahumada, E., Caffee, M., Masana, E., 2013. Timing and nature of alluvial fan and strath terrace formation in the Eastern Precordillera of Argentina. Quaternary Science Reviews 80, 143–168.

Ishiyama, T., Mueller, K., Togo, M., Okada, A., Takemura, K., 2004. Geomorphology, kinematic history, and earthquake behavior of the active Kuwana wedge thrust anticline, central Japan. Journal of Geophysical Research 109, B12408. http://dx.doi.org/10.1029/2003JB002547.

Ishiyama, T., Mueller, K., Sato, H., Togo, M., 2007. Coseismic fault-related fold model, growth structure, and the historic multisegment blind thrust earthquake on the basement-involved Yoro thrust, central Japan. Journal of Geophysical Research 112, B03S07. http://dx.doi.org/10.1029/2006JB004377.

Johnson, K., Johnson, A., 2002. Mechanical models of trishear-like folds. Journal of Structural Geology 24, 277–287. http://dx.doi.org/10.1016/S0191-8141(01)00062-1.

Jordan, T., Isacks, B., Allmendinger, R., Brewer, J., Ramos, V., Ando, C., 1983. Andean tectonics related to geometry of subducted Nazca plate. Geological Society of America Bulletin 94, 341–361.

Kelson, K., Kang, K., Page, W., Lee, C.-T., Cluff, L., 2001. Representative styles of deformation along the Chelungpu fault from the 1999 Chi-Chi (Taiwan) earthquake: geomorphic characteristics and responses of Man-made structures. Bulletin of the Seismological Society of America 91 (5), 930–952.

Lee, J., Rubin, C., Mueller, K., Chen, Y., Chana, Y., Sieh, K., Chu, H., Chen, W., 2004. 2004. Quantitative analysis of movement along an earthquake thrust scarp: a case study of a vertical exposure of the 1999 surface rupture of the Chelungpu fault at Wufeng. Western Taiwan Journal of Asian Earth Sciences 23, 263–273.

Lin, M., Wang, C., Chen, W., Yang, C., Jeng, F., 2007. Inference of trishear-faulting processes from deformed pregrowth and growth strata. Journal of Structural Geology 29, 1267–1280.

Liu-Zeng, J., Zhang, Z., Wen, L., Tapponnier, P., Sun, J., Xing, X., Hu, G., Xu, Q., Zeng, X., Ding, L., Ji, C., Hudnut, K., van der Woerd, J., 2009. Co-seismic ruptures of the 12 May 2008, Ms 8.0 Wenchuan earthquake, Sichuan:East–west crustal shortening on oblique, parallel thrusts along the eastern edge of Tibet. Earth and Planetary Science Letters 286, 355–370.

McCalpin, J., Carver, G., 2009. Paleoseismology of Compressional tectonic environments. In: McCalpin, J. (Ed.), Paleoseismology. Academic Press, San Diego, pp. 315–419.

Mueller, K., Suppe, J., 1997. Growth of Wheeler Ridge anticline, California: geomorphic evidence for fault-bend-folding behavior during earthquakes. Journal of Structural Geology 19, 383–396.

Ramos, V., 1988. The tectonics of the Central Andes; 30° to 33°S latitude. In: Clark, S., Burchfiel, C. (Eds.), Processes in Continental Lithospheric Deformation, Geological Society of America Special Paper, Boulder, CO, vol. 218, pp. 31–54.

Ramos, V., Cristallini, E., Pérez, D., 2002. The Pampean flat-slab of the central Andes. Journal of South American Earth Sciences 15, 59–78.

Salomon, E., Schmidt, S., Hetzel, R., Mingorance, F., Hampel, A., 2013. Repeated folding during late Holocene earthquakes on the La Cal thrust fault near Mendoza city (Argentina). Bulletin of the Seismological Society of America 103 (2), 936–949. http://dx.doi.org/10.1785/0120110335.

Schmidt, S., Hetzel, R., Mingorance, F., Ramos, V., 2011. Coseismic displacements and Holocene slip rates for two active thrust faults at the mountain front of the Andean Precordillera (~33°S). Tectonics 30. http://dx.doi.org/10.1029/2011TC002932. TC5011.

Schmidt, S., Tsukamoto, S., Salomon, E., Frechen, M., Hetzel, R., 2012. Optical dating of alluvial deposits at the orogenic front of the Andean Precordillera (Mendoza, Argentina). Geochronometria 39, 62–75. http://dx.doi.org/10.2478/s13386-011-0050-5.

Schoenbohm, L., Costa, C., Brooks, B., Bohon, W., Gardini, C., Cisneros, H., 2013. Fault interaction along the central Andean thrust front: the Las Peñas thrust, Cerro Salinas thrust and the Montecito anticline. In: Eos Transactions Am. Geoph. Union, vol. 94. Fall Meet. Suppl., Abstract T31D-2543.

Suppe, J., Medwedeff, D., 1990. Geometry and kinematics of fault-propagation folding. Eclogae Geologicae Helvetiae 83 (3), 409–454.

Takao, M., Ueta, K., Annaka, T., Kurita, T., Makase, H., Kyoya, T., Kato, J., 2014. Reliability improvement of probabilistic fault displacement hazard analysis (in Japanese). Journal of Japan Association for Earthquake Engineering 14 (2), 16–36.

Vazquez, F., Costa, C., Gardini, C., 2015. In: Anomalías del drenaje y corrimientos ciegos en el piedemonte de la sierra de Las Peñas, Precordillera de Mendoza, presented at the 16th Reunión de Tectónica, Acta de resúmenes, pp. 213–214. ISBN 978-987-3667-17-6.

Woodward, N., Boyer, S., Suppe, J., 1989. In: Balanced Geological Cross-sections: an Essential Technique in Geological Research and Exploration, Presented at 28th International Geological Congress, Washington, DC, p. 132.

Zehnder, A., Allmendinger, R., 2000. Velocity field for the trishear model. Journal of Structural Geology 22, 1009–1014.